Journal of Cleaner Production 230 (2019) 945–955

Contents lists available at ScienceDirect

Journal of Cleaner Production

journal homepage: www.elsevier.com/locate/jclepro

Self-compacting recycled aggregate concrete using out-of-service railway superstructure wastes

Jose Sainz-Aja, Isidro Carrascal, Juan A. Polanco, Carlos Thomas*, Israel Sosa, Jose Casado, Soraya Diego

LADICIM (Laboratory of Science and Engineering of Materials), University of Cantabria. E.T.S. de Ingenieros de Caminos, Canales y Puertos, Av. Los Castros 44, Santander, 39005, Spain

ARTICLE INFO

Article history:
Received 20 January 2019
Received in revised form
5 April 2019
Accepted 29 April 2019
Available online 10 May 2019

Keywords:
Self-compacting concrete
Recycled aggregate concrete
Slab track
Ballast
Sleepers
Durability

ABSTRACT

Slab track is replacing obsolete ballasted track. This work proposes crushing out-of-service ballast and sleepers for use as aggregates for constructing the slab track. Three kinds of recycled self-compacting concretes were designed; the first one with aggregates from crushed ballast, the second one with aggregates from crushed sleepers and the third one with both kinds of aggregates in the proportion they appear in the track. The mechanical and durability properties of these concretes were analysed. The durability test was focused on freeze-thaw and drying-wetting cycles. The results obtained lead to the conclusion that out-of-service track could be used to build the new one, closing the loop.

© 2019 Elsevier Ltd. All rights reserved.

1. Introduction

During 2016, a total of 2533 million tons of waste were generated in the European Union. Almost 36.4 %wt. of which came from construction. The large volume of construction and demolition waste (C&DW) generated makes the situation unsustainable. Poon et al. estimated that in 8 years landfills in China will be saturated (Poon and Chan, 2007). Due to the large volume of these wastes generated each year, it is of great interest to find a use that allows them to be reused instead of being collected in landfills. Their use for manufacturing recycled aggregate concretes (RAC) was proposed to provide added value for these wastes.

The use of RAC is relatively widespread nowadays, since it is used in different concrete construction projects (Poon et al., 2002; Thomas et al., 2016), although the properties of the specific RAs must be analysed before mixing concrete because there are important differences compared to natural aggregates due to the presence of adhered mortar, such as higher absorption coefficient or lower density (Silva et al., 2014; Padmini et al., 2009). Consequently, RACs have some disadvantages such as a higher porosity, poorer freeze-thaw resistance (Omary et al., 2016) or less compressive strength than traditional concrete (Tabsh and Abdelfatah, 2009). The use of fine recycled aggregates (FRA) has also been studied, and it has been shown that their durability behaviour and mechanical properties are poorer (Evangelista and de Brito, 2010; Ravindrarajah et al., 1987). For these reasons, standards such as EHE-08 or EN 13242 (Fomento, 2008; E.N. 13242:2002+A1:2008, 2002) impose some limitations on the use of coarse aggregates and ban the use of FRA.

For approximately 130 years, railway traffic has been carried mostly on ballasted track. The more demanding requirements, due to the characteristics of high-speed networks, higher axle loads and higher train frequencies have pushed the capacities of the ballasted track to the limit. This is reflected in the intense maintenance work required by ballasted high-speed lines. To obtain a more cost-efficient railway superstructure, track systems without ballast, also called concrete slab track systems, have become popular.

Slab track leads to an important economic saving in maintenance and provides better mechanical behaviour, although it requires a higher initial investment and more time to build (Esveld, 1999). There are comparative studies of traditional track, formed by ballast and sleepers, and slab track, analysing economic aspects

* Corresponding author.
E-mail address: thomasc@unican.es (C. Thomas).

https://doi.org/10.1016/j.jclepro.2019.04.386
0959-6526/© 2019 Elsevier Ltd. All rights reserved.

such as the reduction in maintenance costs or the life cycle cost and technical aspects such as weight reduction or higher lateral track resistance (Tayabji and Bilow, 2001). K. Ando et al. (Ando, 2001) estimated that the extra cost of slab track construction instead of ballasted track could be recovered in about 2–6 years due to its lower maintenance costs.

The use of self-compacting concrete (SCC) has become popular during recent years. It is not only due to the noise reduction during the construction phase, as a consequence of avoiding vibration, but it also reduces the duration of construction, which will be reflected in lower construction costs.

The idea of combining RA and SCC, has been analysed previously by other authors obtaining good results. S. C, Kou and C.S. Poon (Kou and Poon, 2009) found that the properties of the SCC manufactured with river sand and FRA showed only slight differences. Pereira de Oliveira (Pereira-De-Oliveira et al., 2014) analysed the durability behaviour of SCC made with RA and found that the presence of RA did not significantly affect the water permeability and slightly decreased the water capillarity.

This paper, once a ballasted track is obsolete and it is to be replaced, proposes crushing the ballast and the sleepers, and using them as RA and FRA for the construction of slab track. If it is done in this way, the old track will be used to build the new one, closing the loop. To analyse this idea, three kinds of recycled and self-compacting concrete were designed, the first one with aggregates from crushed ballast, the second one with aggregates from crushed sleepers and the third one, with both kinds of aggregates in the proportion they appear in the track.

This idea could provide an economic benefit, on the one hand, from the saving in the purchase of the new materials and, on the other hand, from the savings in the transport to the landfill of the removed material. In addition, it could generate an environmental benefit for the same reasons: the reduction in the use of natural resources and the reduction in the volume of waste after the withdrawal of the obsolete ballasted track.

To obtain the maximum reduction in CO2 emissions in the construction of the slab track some measures were taken. On the one hand, RAC was used (Xiao et al., 2018; Alnahhal et al., 2018; Azúa et al., 2019), on the other hand, the cement used for the concrete contains nearly 50% of clinker and 50% fly ash (Uthaman et al., 2018; Tosti et al., 2018).

2. Materials and methods

2.1. Cement

A CEM IV (V) 32.5 N type cement was used, with a density of 2.85 g/cm^3 obtained according to UNE 80103 (U.N.E. 80103:2013, 2013) and a Blaine specific surface area of 3885 cm^2/g obtained according to EN 196–6 (E.N. 196–6:2010, 2010) supplied by Cementos Alfa (Spain). This type of cement contains approximately 50% of clinker substituted by fly ash, which means 50% less clinker than a CEM I type and provides adequate mechanical properties for a slab track (She et al., 2018). The chemical composition of the cement is shown in Table 1. Furthermore, the use of this cement type with a high clinker replacement ratio reduces the environmental footprint of the concrete (Uthaman et al., 2018; Tosti et al., 2018).

2.2. Superplasticizer additive

In order to obtain the desired fluidity of the self-compacting concrete, a superplasticizing additive, MasterGlenium® ACE 450 BASF, was used. To define the optimal quantity of additive, the Marsh cone test was performed according to ASTM C939-97 (ASTM), with the modification that not only 200 ml were tested but also 500, 750 and 1000 ml were analysed in order to obtain more robust and measurable results.

2.3. Recycled aggregates

To produce the RA, on the one hand, out-of-use ballast and, on the other hand, out-of-use sleepers were crushed and sieved. The procedure begins with the collection of the out-of-service elements; see Fig. 1 (A) out-of-service ballast collection and (B) out-of-service sleeper collection. The crushing process is shown in Fig. 1(C) and (D).

Railway superstructure wastes include wooden sleepers, metal fixing elements and in most cases natural basaltic aggregates of ballasted track, although in some countries other materials are used which fulfil the physical/mechanical requirements. Therefore, the nature of the wastes generated depends on availability of locally-sourced aggregates that fulfil these requirements. This research analyses the utility of concrete sleepers and basaltic ballast exclusively.

The original ballast crushed to obtain the RA-B has is basaltic and fulfils the requirements described in the Spanish standard (M.

Fig. 1. (A) Ballast waste generation in the renewal of ballast track left. (B) Out-of-service concrete sleepers. (C) Crushing procedure to obtain the recycled aggregates. (D) Crushing procedure detail.

Table 1
Chemical composition of the cement.

Composition [%wt.]								
	CaO	SiO_2	Al_2O_3	Fe_2O_3	MgO	K_2O	SO_3	Ignition loss
Cem IV	35.54	41.10	13.33	4.44	1.24	1.39	1.26	1.70

de fomento 7735, 2006). However, the ballast studied was obtained after renewal of the track, as a consequence of its geometrical parameters.

The sleepers crushed to obtain the aggregates, when they were installed, fulfilled the requirements for sleepers of the Spanish state-owned railway infrastructure managers under the responsibility of the Ministry of Public Works and Transport (ADIF). The concrete had compressive strength greater than 65 MPa. This value of compressive strength will provide the aggregates with the required properties for a RC. Akbarnezhad et al. (2013) concluded that the parent concrete properties have a relevant importance in the RC properties.

This out-of-service material was provided by ADIF. The crushing procedure was carried out in the waste treatment plant VALORIA RESIDUOS S.L. (Spain) using a portable jaw crusher which was able to separate the steel from the concrete. Once the material was crushed, 3 sieves were used to separate each aggregate into three different sizes: 0–2 mm, 2–5 mm and 5–15 mm, see Table 2 and Fig. 2. Three different types of concretes were mixed with these six aggregate fractions. The first of them is made only with RA from crushed ballast (RC-B), the second with RA from crushed sleepers (RC-S) and the third with a mixture of aggregates from crushed ballast and aggregates from crushed sleepers in the track proportion (RC-M).

These RAs were subjected to mechanical and geometrical tests in order to guarantee that they could be used to form a self-compacting concrete.

The aggregate properties obtained were the densities according to EN 1097–3 (British Standards Institution, 1998), the absorption coefficient according to EN 1097–6 (EN 1097–6:2014, 2014), the grading curve according to EN 933–1 (E.N. 933–1:2012, 2012), the flakiness index according to EN 933–3 (E.N. 933–3:2012, 2017) and the Los Angeles abrasion test according to EN 1097–2 (E.N. 1097–2:2010, 2010).

Representative samples of 1 kg of coarse aggregates were isolated in order to visually identify impurities such as wood or ceramics. The maximum quantity of detected impurities was always less than 1 %wt.

The main properties of the RA are shown in Table 3 and the grading curves are shown in Fig. 3.

For both recycled aggregates, from the crushed ballast and the crushed sleepers, there is an increase in density with the reduction of the sand particle size, from 2.73 g/cm^3 (RA-BS) to 2.89 g/cm^3 (RA-FBS) for the crushed ballast sand, and from 2.51 g/cm^3 (RA-SS) to 2.62 g/cm^3 (RA-FSS) for the crushed sleeper sand. The density of the ballast aggregate is always higher than the sleeper one.

In the case of coarse aggregates, the density of the RA-SCA is 5% less than RA-BCA. As can be expected (Silva et al., 2014; Padmini et al., 2009), the absorption coefficient of RA-SCA is 2.7 times higher than of RA-BCA. As the Los Angeles coefficient shows, RA-SCA has poorer mechanical properties than RA-BCA. However, the flakiness index of the RA-BCA is nearly three times higher than RA-SCA. Zega et al. (2010) compared the physical-mechanical properties of natural aggregate (NA) and RA and found similar differences in the flakiness index. In this case, the apparent and bulk specific gravity, absorption and Los Angeles abrasion coefficients clearly indicate that RA-SCAs are of a lower quality than RA-BCAs because of the adhered mortar they contain (Soares et al., 2014). Likewise, the aggregate skeleton of the concrete made with the RA-BCA will be less compact due to the flakiness index.

Table 2
Aggregate identification.

Code	Waste	Size [mm]
RA-FBS	Ballast	[0–2]
RA-BS	Ballast	[2–5]
RA-BCA	Ballast	[5–15]
RA-FSS	Sleepers	[0–2]
RA-SS	Sleepers	[2–5]
RA-SCA	Sleepers	[5–15]

2.4. Mix proportions

The mix proportions were defined in three sub steps. In the first one, the quantity of superplasticizer additive was chosen (this process was defined in section 2.2). In the second step, 10 mortar mixes per kind of concrete were manufactured to determine the relation between the different sands according to mortar workability and compressive strength. For the final concrete mix proportions, the quantity of cement was fixed at 500 kg/m^3. The final mix proportions are shown in Table 4. The aggregates used for the manufacture of the concrete were at temperature and humidity corresponding to the laboratory conditions. The temperature was in all cases 21 ± 3 °C and the humidity in all cases less than 0.5%.

RC-B and RC-S were designed using 100% of incorporation of RA and the RC-M using a proportion of 6/7 RA form ballast and 1/7 RA from sleepers. The mix proportions are shown in Table 4.

It can be observed that RC-B has a higher w/c ratio, although it could be expected that the use of RA-S needs more water as a consequence of the higher absorption of the aggregates (Evangelista and de Brito, 2010). However, due to the higher flakiness index of the RA-B, a higher volume of mortar and water is needed to obtain self-compacting concrete. Medina et al. (2014) concluded that concretes with a low w/c ratio through the use of superplasticizer additive provide higher mechanical strength, low capillarity and absorption and thus better durability. Matias et al. and Saravana et al. (Saravana Kumar and Dhinakaran, 2012; Matias et al., 2014) concluded that the use of superplasticizer is a significant component in producing good quality RAC.

2.5. Workability

The workability tests on self-compacting concrete were carried out according to their corresponding standards. The results of the tests were compared with EN 206 (E.N. 206:2013+A1:2016, 2018) and also with The European Guidelines for Self-Compacting Concrete (Efnarc and Efnarc, 2002). The tests which were carried out to measure the workability of the concretes were: the slump flow test, according to EN 12350–8 (E.N. 12350–8:2010, 2011) which takes EN 12350–2 (E.N. 12350–2:2009, 2009) as a reference; the L-box test according to the EN 12350–10 (E.N. 12350–10:2010, 2015) standard, using the model B bars for the L-Box test; the V-funnel test was carried out according to EN 12350–9 (E.N. 12350–9:2010, 2011); and the GTM screen stability test according to EN 12350–11 (E.N. 12350–11:2010, 2010). In addition, the fresh concrete density was measured. This concrete density was measured in 10 different samples per mix proportion. The methodology to determine the concrete density consisted in weighing the mould of the cubic concrete sample both before and after introducing the concrete into the mould. As the volume of the mould is known, it was possible to determine the density of each sample.

2.6. Tests on hardened concrete

Once the mix proportions were established for a self-compacting concrete, different size specimens were manufactured in order to characterize the main properties of the hardened concrete, such as the uniaxial compressive strength, the modulus of elasticity and the durability.

Fig. 2. RA produced using ballast and sleepers.

Table 3
Coarse aggregate properties.

Material	Apparent specific gravity	Bulk specific gravity	Absorption coefficient	Los Angeles coefficient	Flakiness index
	[g/cm^3]	[g/cm^3]	[% wt.]	[%]	[%]
RA-BCA	2.48	2.37	1.9	20	14
RA-SCA	2.34	2.09	5.1	36	5

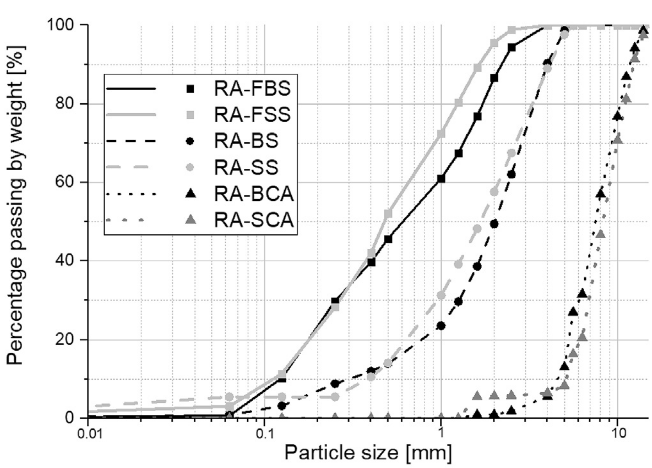

Fig. 3. Aggregate grading curves.

Table 4
Mix proportions (by m^3).

Material	RC-B	RC-S	RC-M
Water (kg)	225	200	221
Cement (kg)	500	500	500
Superplasticizer additive (kg)	10	10	10
RA-FBS (kg)	790	–	677
RA-BS (kg)	320	–	274
RA-BCA (kg)	522	–	447
RA-FSS (kg)	–	690	98
RA-SS (kg)	–	283	40
RA-SCA (kg)	–	587	83
Water/cement ratio	0.45	0.40	0.44
% sand [0–2 mm] of total sand	70	70	70
% coarse aggregate of the total aggregates	35	40	36
% superplasticizer additive/cement	2.00	2.00	2.00

2.6.P. hysical properties

The bulk densities were obtained according to EN 12390–7 (E.N.

12390–7:2009, 2009) and the accessible porosity and the absorption coefficient were obtained according to UNE 83980 (U.N.E. 83980:2014, 2014).

2.6.2. Mechanical properties

To obtain the mechanical properties of the three types of concrete, the uniaxial compressive strength test and modulus of elasticity test were performed at different ages in order to analyse the evolution of these properties. The uniaxial compressive strength tests were performed according to the EN 12390–3 and EN 13290–3/AC (U.-E. 12390–3:2009, 2009; E.N. 12390–3:2099/AC, 2011, 2011) standards, using cubes of 100 mm side. These tests were performed at the ages of 1, 2, 3, 5, 7, 28, 90 and 180 days. The initial and stabilized secant moduli of elasticity tests was performed according to EN 12390–13 (E.N. 12390–13:2013, 2014) at the ages of 7, 28, 90 and 180 days using cylindrical specimens of 200 mm height and 100 mm diameter.

2.6.3. Wear resistance

The wear resistance was measured following EN 1338 (E.N. 1338:2003, 2004). These tests were performed at the age of 90 days. The test samples for the wear tests were cut to perform the tests on an interior surface of the sample.

2.6.4. Durability

As is well known, the presence of fly ash means that the concretes continue to undergo important changes until the age of 90 days (Kou and Poon, 2012), so all the durability tests were carried out at the age of 90 days rather than 28 days in view of the large quantity of fly ash present in the cement.

To analyse the long-term life of the concrete, the first step was to measure the permeability of the concrete. This parameter was obtained in two ways: the oxygen permeability test, according to the UNE 83966, UNE 83981 and UNE 83981-ERRATUM (U.N.E. 83966:2008, 2008; U.N.E. 83981:2008, 2008; U.N.E. 83981:2008, 2011) standards; and the water permeability test according to the EN 12390–8 and EN 12390–8/M (E.N. 12390–8:2009, 2009; U.-E. 12390–8:2009/1M:2011, 2011) standards. 3 cylindrical standardized test specimens of 150 mm diameter and 300 mm height were cut into 3 cylinders of approximately 100 mm of height. The top and the bottom of all the samples were removed by cutting. These 9 subsamples were used for the oxygen and water permeability testing.

To analyse the shrinkage, specimens of 300 × 50 × 50 mm were prepared and the variation of length with time was measured according to UNE 83318 (U.N.E. 83318:1994, 1994).

Freeze-thaw cycle tests were performed according to the UNE-CEM/TS 12390-9EX (C. 12390–9:2006, 2008) standard, using the alternative method of the cubes, with the modification that the samples were tested at the age of 90 instead of 28 days. In addition, the freeze time was increased to 42 h in order to reach −15 °C.

Drying-wetting cycle tests were performed taking as a reference EN 14066 (E.N. 14066, 2014). During these tests, 100 cycles were performed of 8 h sunk in water and 16 h in the oven at 70 °C. The evolution of the weight and the ultrasound crossing time were measured to analyse the damage suffered by the samples. In addition, after these 100 cycles, the samples were subjected to uniaxial compression testing to measure the residual compressive strength. This parameter of residual compressive strength was defined as the percentage of compressive strength retained at the end of the 100 cycles.

3. Results and discussion

3.1. Workability

In Fig. 4 (A) the slump flow test of the RC-B can be seen. There is minimum segregation, which can be detected due to the presence of a water/paste/mortar ring beyond the coarse aggregate. In addition, it can be seen that there are coarse aggregates even at the edge of the flow spread. In Fig. 4 (B), the slump flow of the RC-S can be seen, here, in contrast, there is no segregation, as there is no water/paste/mortar ring beyond the coarse aggregate. In addition, a higher quantity of coarse aggregate could be observed at the edge of the flow. The cause of the higher quantity of aggregates is the higher viscosity of the mortar produced by the lower w/c ratio. In addition, it can be appreciated that the perimeter of the flow spread is much more regular in the RC-B, leading to greater thixotropic behaviour reflected in a lower value in the V funnel test. Fig. 4 (C) shows the slump flow of the RC-M. In this case, there is no segregation, but the quantity of coarse aggregates at the edge of the flow spread is between RC-B and RC-S.

Table 5 shows the workability test results.

While the increase in RA from crushed concrete normally reduces the w/c ratio and so the workability of the concrete (Carro-López et al., 2015; Aslani et al., 2018), Barbudo et al. (2013) concluded that combining the use of superplasticiser additive with RA could address the need for adding extra water to obtain the same workability, thus obtaining an advantage in the properties of the hardened concrete.

In this case, due to the geometry of the particles, observed in the flakiness index, RC-S obtains the best results in the slump flow and the L-box test.

3.2. Tests on hardened concrete

Once it was proved that the workability of the concrete was adequate, several test specimens were manufactured in order to analyse their hardened state properties. The physical, mechanical and durability properties were analysed.

3.2.P. hysical properties

The physical properties are shown in Table 6.

As can be expected, the values of density are lower in RC-S as a consequence of the lower density of its aggregates despite its lower w/c ratio. The absorption and porosity are higher in RC-S because of the higher absorption of the aggregates (Thomas et al., 2013). The RC-M properties are situated between those of the RC-B and the RC-S.

The presence of RA tends to lower the density value. Otherwise, lower values of effective w/c ratio could increase the density of the concrete (Zega et al., 2010; Oliván).

The values of density and absorption of RAC are similar to those of other authors with a 100% of aggregate substitution (Zega and Di Maio, 2011).

3.2.2. Mechanical properties

Fig. 5 shows the results of the evolution of the average compressive strength in four different samples per age.

The concrete with the highest compressive strength is the RC-S one, due to the lower effective w/c ratio. RC-B obtained the lowest results despite the poorer tribological properties of these aggregates. RC-M results are between the RC-B and the RC-S, as could be expected. All the mix proportions are always above 37 MPa at 28 days, which is the requirement for slab track concrete according to the company Rail One © for its most popular slab track typology, “Rheda 2000”. In addition, it was possible to reach this strength due

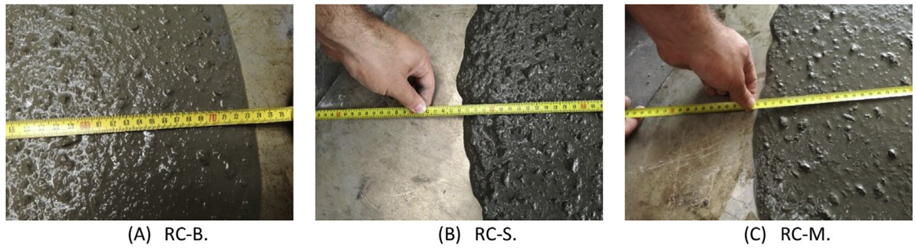

Figure 4. Shows details of the workability of the concrete.

Table 5
Workability test results.

Test				EN 206-9			EFNARC		
	RC-B	RC-S	RC-M	RC-B	RC-S	RC-M	RC-B	RC-S	RC-M
Slump flow SF [mm]	700	730	800	SF2	SF2	SF3	OK	OK	OK
T_{50cm} test [s]	2	2.5	2	VS2	VS2	VS2	OK	OK	OK
L-box test method	0.90	0.90	0.95	PL1	PL1	VPL1	OK	OK	OK
V funnel test [s]	7.5	13.5	6.0	VF1	VF2	VF1	OK	No OK	OK
GTM stability test [%]	1.0	8.8	8.8	SR2	SR2	SR2	OK	OK	OK
Fresh density [g/cm^3]	2.4	2.3	2.4	–	–	–	–	–	–

Table 6
Physical properties of the different concretes.

Mix	Bulk specific gravity [g/cm^3]	Apparent specific gravity [g/cm^3]	Bulk saturated surface dry [g/cm^3]	Absorption coefficient (%wt.)	Accessible porosity (%vol.)
RC-B	2.27	2.51	2.37	4.1	9.2
RC-S	2.12	2.35	2.22	4.8	10.1
RC-M	2.26	2.50	2.36	4.2	9.5

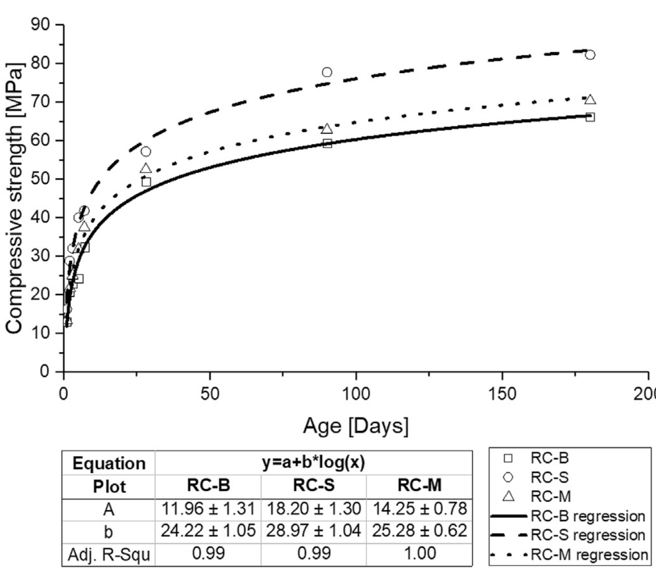

Fig. 5. Evolution of the compressive strength of the RC-B, RC-S and RC-M.

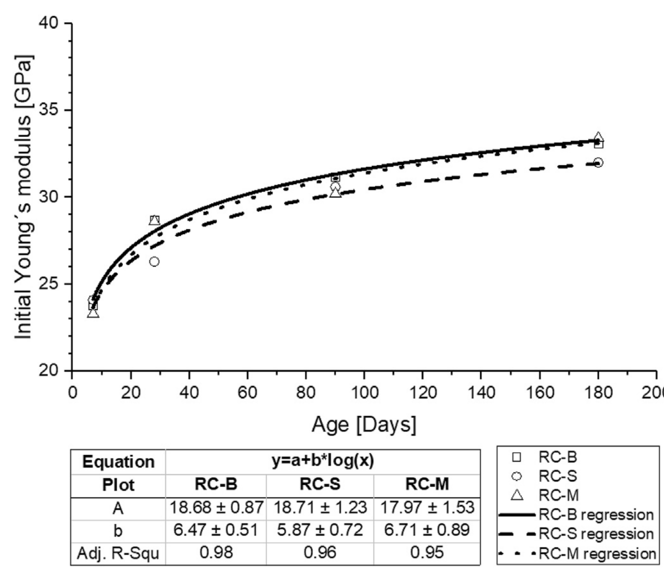

Fig. 6. Evolution of the initial modulus of elasticity of the RC-B, RC-S and RC-M.

to the good quality of the crushed ballast and sleepers. Tabsh et al. (Tabsh and Abdelfatah, 2009) demonstrated the influence of quality of the parent concrete on the quality of RA.

Two different moduli of elasticity were measured. The results of the evolution of the average of two different samples per age of these parameters are shown in Fig. 6 and Fig. 7. There are no great differences between the distinct concretes. The modulus of elasticity of RC-B is higher due to the greater stiffness of its aggregates. RC-S had similar values to other RAC moduli of elasticity with the same w/c ratio (Etxeberria et al., 2007), generally being lower than concrete with NA (Kou et al., 2007; Dapena et al., 2011).

3.2.3. *Wear resistance*

The wear resistance results are shown in Fig. 8.

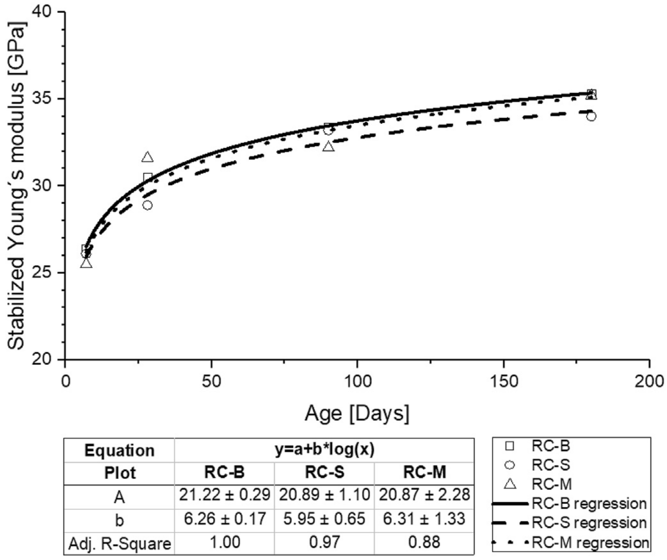

Fig. 7. Evolution of the stabilized modulus of elasticity of the RC-B, RC-S and RC-M.

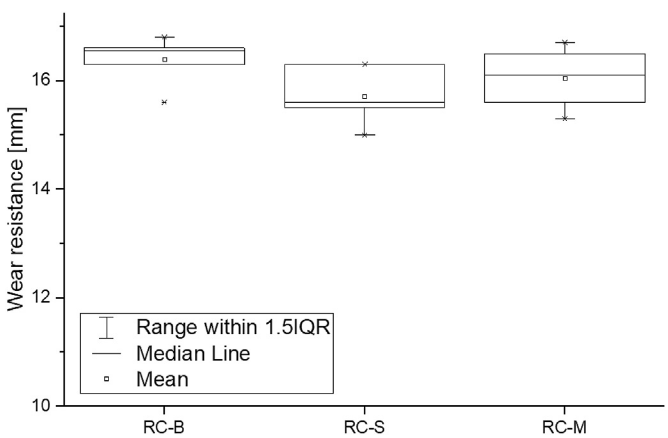

Fig. 8. Evolution of the wear resistance of the RC-B, RC-S and RC-M.

The values of the wear resistance are quite similar in all the mix proportions, but slightly higher in the RC-B. In the three mix proportions all the values are lower than the most restrictive value defined in the EN 1338:2003 (E.N. 1338:2003, 2004), which is 20 mm. The RA's effect on wear resistance is not completely clear: some authors (de Brito, 2010; Abreu et al., 2018) found that the presence of RA reduces the wear resistance while others (Bravo et al., 2015) found an increment in the wear resistance when coarse RA were used. The lower w/c ratio causes the increase of the wear resistance (Laplante et al., 1991; Warudkar et al., 2018). Again, the lower w/c ratio provides better RC-S qualities than RC-B ones.

3.2.4. Durability

Permeability is a reliable parameter for measuring the durability of concrete because it is the property responsible for the penetration of any agent that could damage the concrete. The results of both oxygen permeability and water permeability are shown in Table 7. The lowest values of oxygen permeability are in RC-S, and the highest ones are in RC-B. It is well known that the presence of RAs does not really affect the permeability of concrete (Pereira-De-Oliveira et al., 2014), and a lower water/cement ratio provides a lower permeability to RC-S. It is also well known that the use of fly ash will help to reduce the permeability of a concrete (Kou and Poon, 2012), for this reason, all the mix proportions provided good results. These values of permeability are low, so good durability behaviour can be expected.

Table 7
Permeability of the concrete.

Concrete	Oxygen permeability coefficient	Water permeability	
	[m^2]	Max penetration [mm]	Mean penetration [mm]
RC-B	3.0 E−17	50	40
RC-S	1.5 E−17	20	20
RC-M	1.6 E−17	40	20

The criterion of similar consistency in fresh state has the consequence that RC-B displays a higher water/cement ratio than RC-S. This explains that RC-B's permeability both to water and gases is the highest of all.

The water penetration in the RC-B is the highest, even higher than expected, but for all of the mix proportions it is higher than the values defined in standards such as EHE-08 (Fomento, 2008). The reason for this high penetration is the presence of impurities and the higher effective w/c ratio.

The variation in the length of the concrete specimens is plotted in Fig. 9.

The RC-B samples suffer the highest shrinkage strain and the RC-S the lowest. Usually, the presence of aggregates from RAC increases the shrinkage (Domingo-Cabo et al., 2009), but as can be noted from the figure above, the RC-B samples undergo more shrinkage strain due to the higher w/c ratio of these mixes (Zega and Di Maio, 2011). The value of the shrinkage obtained for the RC-Ss are similar to the values obtained by Nyok Yong Ho et al. (2013), being higher than usual for a concrete with NA, although within the recommended limits for Standards Australia (SA) "Concrete structures" (Standards Australia, 2009), which fixes the range of shrinkage values for normal concretes at 0.08%.

The evolution of the loss of mass during the freeze-thaw accelerated ageing is plotted in Fig. 10. RC-B shows two different phases or behaviours; before cycle 10 a pronounced loss of mass is observed, while from this point a linear variation of the weight with

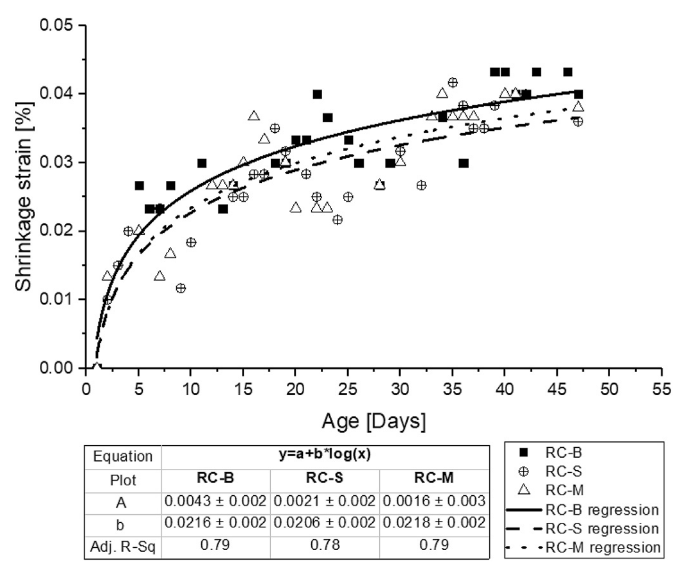

Fig. 9. Evolution of the shrinkage of the RC-B, RC-S and RC-M.

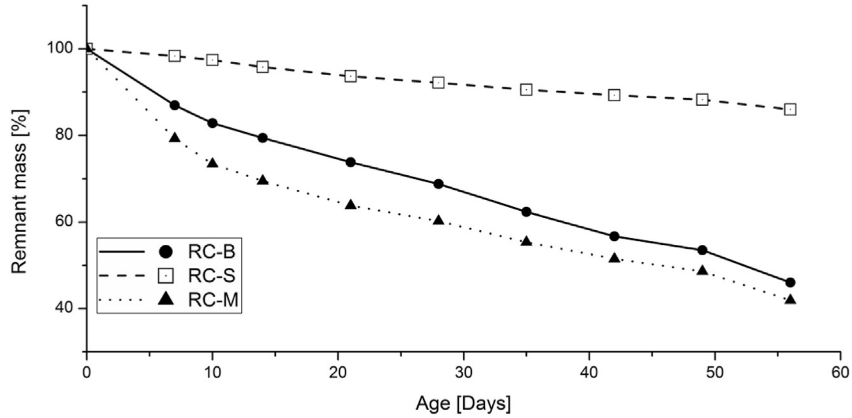

Fig. 10. Evolution of the freeze-thaw mass evolution of RC-B, RC-S and RC-M.

cycles is observed. This higher loss of mass in the first phase is a consequence of the geometry of the samples. The initiation of the loss of mass is first detected at the corners and then at the edges of the cube. With 56 cycles, the samples undergo a loss of mass of nearly 50 %wt. RC-S shows a linear variation of the mass with cycles from the first to the last cycle. With 56 cycles, the samples undergo a loss of mass of nearly 10%wt. RC-M shows a higher loss of mass than RC-B and RC-S. In RC-M the same phases or behaviour as in RC-B are detected. However, in this case the loss of mass in the first phase is more pronounced than with RC-B. Again from cycle 10, linear behaviour is observed, with a total loss of mass after 56 cycles of nearly 60%wt.

Fig. 11 shows the specimens tested after 56 freeze-thaw cycles of accelerated ageing. It can be seen that the RC-B has undergone intermediate damage, having lost an important part of its original geometry. It can be appreciated that RC-S has suffered less damage, maintaining its cubic shape. For the same concrete, an external mortar degradation has been observed as a consequence of its low permeability.

Both the concrete with ballast aggregate and the mixed one undergo very similar mass losses, the damage observed in the mixed one being slightly greater. RC-S suffers the least damage under freeze-thaw, as a consequence of its lower rigidity and greater capacity to absorb microdeformations.

Amorim Junior et al. (Júnior et al., 2017) observed that with 15% replacement of the coarse natural aggregate by the coarse recycled aggregate there is greater durability to the expansion stresses of the water. Alan Richardson et al. (2011) found that RACs are 68% more durable for freeze-thaw cycles than NAs. The RC-Ms, combining both types of aggregates, show the highest damage as a consequence of the weakest part of the RC-B, its mortar, and of the RC-S, its higher aggregate absorption (Alexandridou et al., 2018). Water shows greater capacity to flow through RC-M concrete and cracks it when it freezes. It can also be appreciated that the shape of the samples become spherical as this is the geometrical form with less area per unit of volume, demonstrating the importance of the area in contact with the aggressive environment.

The evolution of mass during the drying-wetting accelerated ageing test is plotted in Fig. 12. The RC-B weight increment during the 100 cycles is negligible. The RC-S undergoes a fast initial increment of mass, until cycle 10. After this, the increment of weight is much slower rising by 1.3% of the initial weight after 100 cycles. The RC-M has an intermediate increment of mass, displaying similar behaviour to the RC-S; a faster increment of weight until cycle 20, and a slower increment which rises by 1.2% after 100 cycles.

There is an increase in weight associated with the absorption because, in the period of oven drying, the (standardized) time is not enough to eliminate all the water absorbed in the previous process. RC-S presents the lowest permeability, both to oxygen and water, and better behaviour under the freeze-thaw cycles. It also has the highest absorption coefficient of all the concretes analysed. This

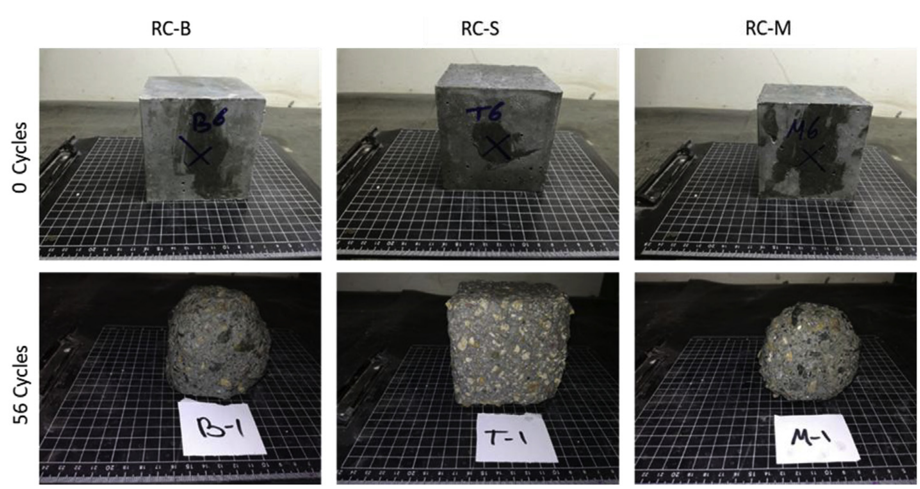

Fig. 11. Freeze-thaw concrete surface deterioration.

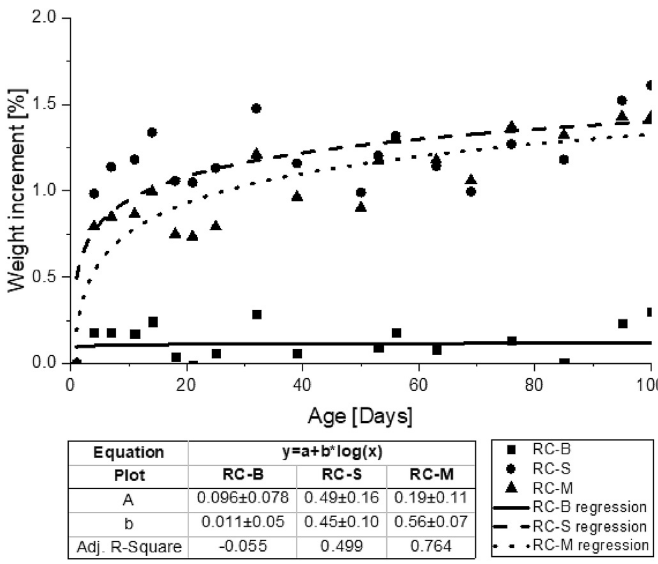

Fig. 12. Drying-wetting test mass evolution of the RC-B, RC-S and RC-M.

concrete is also the one that accumulates most water after the drying-wetting cycles. It is demonstrated that the absorption coefficient depends on the open porosity, which is not directly related to the permeability. That is to say, the combination of a high-density paste and an aggregate with high absorption coefficient can provide concrete with a high absorption coefficient. As shown by Thomas et al. (2013), as recycled concrete evolves (ages greater than 90 days), the difference between the control concrete and the recycled one becomes lower in terms of permeability, while in terms of absorption it remains practically constant. In this case, cements with fly ash and 90-day ageing have been used. Therefore, there has been enough time to reduce the permeability of the paste, although the absorption of recycled aggregates means that the absorption of the concrete is not altered.

The large scatter is a consequence of the sensitivity of the equipment used near to the measured values. In this situation, the uncertainty of the measurement and the scatter is large. In addition, in the case of the drying-wetting test, the $R^2$of the mass evolution of the RC-B curve is extremely low (−0.055). It can be seen that this value is always near to 0 and that the uncertainty of the measurement (similar in the three adjustments) is even higher than the weight increment, which means a poor regression quality.

Table 8
Compressive strength after 100 cycles of drying-wetting.

Concrete	Residual compressive strength	Loss of compressive strength
	[MPa]	[%]
RC-B	52.7	11.3
RC-S	62.3	19.9
RC-M	53.6	13.9

The external appearance of the samples after 100 drying-wetting cycles is shown in Fig. 13. The samples after 100 cycles show no superficial degradation or loss of material. However, all the samples have suffered external discoloration, a slight degradation on the edges and show superficial fissures.

At the end of the 100 cycles, the samples were tested and the loss of compressive strength was analysed. The results are shown in Table 8. The RC-B loses 11% of its compressive strength after 100 cycles. The RC-S loses nearly 20% of its compressive strength after the same accelerated ageing. The RC-M loses 14% of its compressive strength, an intermediate value between the RC-B and the RC-S remaining compressive strength.

During the drying-wetting cycles, a slight external degradation of the faces of the samples is generated. This degradation might cause non-uniform stress distribution during the compressive strength test, decreasing breaking load of the sample. It is possible that this phenomenon affects the more resistant concrete more.

4. Conclusions

The following conclusions are obtained about the recycled concretes manufactured with aggregates from crushed ballast, crushed sleepers and a mix of them:

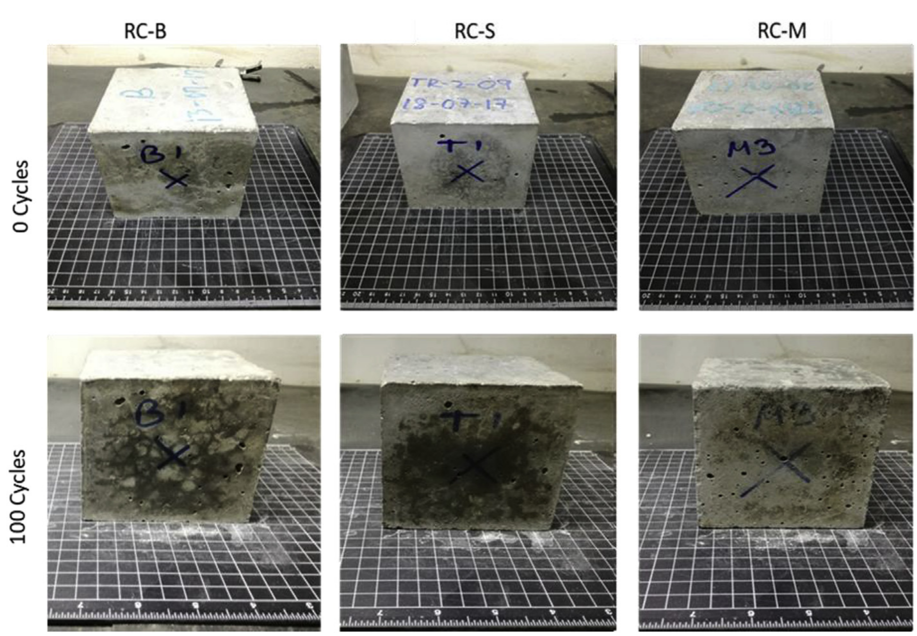

Fig. 13. Drying-wetting concrete surface deterioration.

First, it has been demonstrated that recycling the traditional railway for the production of recycled slab track is possible. This action has two environmental benefits: a more efficient waste disposal and cleaner production.

From the results obtained, it can be deduced that the early age properties of self-compacting recycled concrete have a strong dependence on the geometry of the recycled aggregates. The recycled aggregate from concrete (sleepers) has a more rounded shape that facilitates the fluidity of the fresh mixture, while ballast aggregates with higher flakiness index difficulties the self-compacting of the concrete. In particular, the use of recycled ballast aggregate requires a more fluid cement paste, with higher water/cement ratio, than that of recycled concrete aggregate. For a realistic case, exclusively from the point of view of the early age properties the authors recommend the use of recycled concrete aggregate for the manufacture of slab track due to the better performance compared with the recycled ballast.

It is possible to fulfil the mechanical requirements of slab tracks using recycled aggregate from ballast, concrete and mix of them. However, concretes prepared with recycled concrete aggregate present a more compressive strength due to the lower water/cement ratio, unlike what happens in traditional non-self-compacting concretes.

Regarding the elastic modulus, the influence of recycled aggregate is different than compressive strength. The stiffness of the recycled aggregate from ballast causes that the stiffest concrete is the one that incorporates recycled ballast.

The evolution of the loss of mass during the freeze-thaw accelerated ageing shows two different phases or behaviours: during the initial cycles, a pronounced loss of mass occurs and after that, a linear variation of the weight with cycles is observed. This higher loss of weight in the first phase is a consequence of the geometry of the samples. After the drying-wetting ageing cycles, no superficial degradation or loss of material is detected.

The durability behaviour of the recycled concrete using recycled ballast fulfils the requirements of the standards but the water penetration values are close to the limit. The concrete incorporating recycled concrete aggregate shows high durability indicators due to its lower w/c ratio.

As a final conclusion, it can be say that the use of recycled aggregate from the traditional rail way wastes is technically feasible in recycled concretes. As a consequence of this, and due to the environmental implications, the authors recommend the use of them in the concrete rail slab track.

Acknowledgments

The research received funding sources from the The Spanish Ministry of Economy and Competitiveness for financing the project MAT2014-57544-R and the companies Adif, for the out-of-use ballast and sleepers which are the starting point of this research, and Cementos Alfa, who provided the Cement which has been used to manufacture the concrete.

References

Abreu, V., Evangelista, L., de Brito, J., 2018. The effect of multi-recycling on the mechanical performance of coarse recycled aggregates concrete. Constr. Build. Mater. 188, 480–489. https://doi.org/10.1016/j.conbuildmat.2018.07.178.

Akbarnezhad, A., Ong, K.C.G., Tam, C.T., Zhang, M.H., 2013. Effects of the parent concrete properties and crushing procedure on the properties of coarse recycled concrete aggregates. J. Mater. Civ. Eng. 25, 1795–1802. https://doi.org/10.1061/(ASCE)MT.1943-5533.0000789.

Alexandridou, C., Angelopoulos, G.N., Coutelieris, F.A., 2018. Mechanical and durability performance of concrete produced with recycled aggregates from Greek construction and demolition waste plants. J. Clean. Prod. 176, 745–757. https://doi.org/10.1016/J.JCLEPRO.2017.12.081.

Alnahhal, M.F., Alengaram, U.J., Jumaat, M.Z., Abutaha, F., Alqedra, M.A., Nayaka, R.R., 2018. Assessment on engineering properties and CO2 emissions of recycled aggregate concrete incorporating waste products as supplements to Portland cement. J. Clean. Prod. 203, 822–835. https://doi.org/10.1016/J.JCLEPRO.2018.08.292.

Ando, K., 2001. Development of Slab T racks for Hokuriku Shinkansen Line Tracks 42, 35–41.

Aslani, F., Ma, G., Yim Wan, D.L., Muselin, G., 2018. Development of high-performance self-compacting concrete using waste recycled concrete aggregates and rubber granules. J. Clean. Prod. 182, 553–566. https://doi.org/10.1016/J.JCLEPRO.2018.02.074.

ASTM, ASTM C 939-97, (n.d.).

Azúa, G., González, M., Arroyo, P., Kurama, Y., 2019. Recycled coarse aggregates from precast plant and building demolitions: environmental and economic modeling through stochastic simulations. J. Clean. Prod. 210, 1425–1434. https://doi.org/10.1016/J.JCLEPRO.2018.11.049.

Barbudo, A., de Brito, J., Evangelista, L., Bravo, M., Agrela, F., 2013. Influence of water-reducing admixtures on the mechanical performance of recycled concrete. J. Clean. Prod. 59, 93–98. https://doi.org/10.1016/J.JCLEPRO.2013.06.022.

Bravo, M., de Brito, J., Pontes, J., Evangelista, L., 2015. Mechanical performance of concrete made with aggregates from construction and demolition waste recycling plants. J. Clean. Prod. 99, 59–74. https://doi.org/10.1016/J.JCLEPRO.2015.03.012.

British Standards Institution, 1998. Tests for Mechanical and Physical Properties of Aggregates - Part 3: Determination of Loose Bulk Density and Voids.

C. 12390-9:2006, 2008. Testing Hardened Concrete - Part 9: Freeze-Thaw Resistance - Scaling.

Carro-López, D., González-Fonteboa, B., de Brito, J., Martínez-Abella, F., González-Taboada, I., Silva, P., 2015. Study of the rheology of self-compacting concrete with fine recycled concrete aggregates. Constr. Build. Mater. 96, 491–501. https://doi.org/10.1016/J.CONBUILDMAT.2015.08.091.

Dapena, E., Alaejos, P., Lobet, A., Pérez, D., 2011. Effect of recycled sand content on characteristics of mortars and concretes. J. Mater. Civ. Eng. 23, 414–422. https://doi.org/10.1061/(ASCE)MT.1943-5533.0000183.

de Brito, J., 2010. Abrasion resistance of concrete made with recycled aggregates. Int. J. Sustain. Eng. 3, 58–64. https://doi.org/10.1080/19397030903254710.

Domingo-Cabo, A., Lázaro, C., López-Gayarre, F., Serrano-López, M.A., Serna, P., Castaño-Tabares, J.O., 2009. Creep and shrinkage of recycled aggregate concrete. Constr. Build. Mater. 23, 2545–2553.

Efnarc, F., Efnarc, S., 2002. Specification and Guidelines for Self-Compacting Concrete, Farnham, Surrey GU9 7EN, UK, 0 9539733 4 4. Www.Efnarc.Org.

E.N. 1097-2:2010, 2010. Tests for Mechanical and Physical Properties of Aggregates - Part 2: Methods for the Determination of Resistance to Fragmentation.

EN 1097-6:2014, 2014. EN 1097-6 - Tests for Mechanical and Physical Properties of Aggregates - Part 6: Determination of Particle Density and Water Absorption.

E.N. 12350-10:2010, 2015. Testing Fresh Concrete - Part 10. Self-compacting concrete - L box test.

E.N. 12350-11:2010, 2010. Testing Fresh Concrete - Part 11: Self-Compacting Concrete - Sieve Segregation Test.

E.N. 12350-2:2009, 2009. Testing Fresh Concrete - Part 2. Slump-test.

E.N. 12350-8:2010, 2011. Testing Fresh Concrete - Part 8. Self-compacting concrete - Slump-flow test.

E.N. 12350-9:2010, 2011. Testing Fresh Concrete - Part 9. Self-compacting concrete - V-funnel test.

E.N. 12390-13:2013, 2014. Testing Hardened Concrete - Part 13: Determination of Secant Modulus of Elasticity in Compression.

E.N. 12390-3:2099/AC:2011, 2011. Testing Hardened Concrete - Part 3: Compressive Strength of Test Specimens.

E.N. 12390-7:2009, 2009. Testing Hardened Concrete - Part 7: Density of Hardened Concrete.

E.N. 12390-8:2009, 2009. Testing Hardened Concrete - Part 8: Depth of Penetration of Water under Pressure.

E.N. 13242:2002+A1:2008, 2002. Aggregates for Unbound and Hydraulically Bound Materials for Use in Civil Engineering Work and Road Construction.

E.N. 1338:2003, 2004. Concrete Paving Blocks - Requirements and Test Methods.

E.N. 14066, 2014. Natural Stone Test Methods - Determination of Resistance to Ageing by Thermal Shock.

E.N. 196-6:2010, 2010. Methods of Testing Cement - Part 6. Determination of fineness.

E.N. 206:2013+A1:2016, 2018. Concrete - Specification, Performance, Production and Conformity.

E.N. 933-1:2012, 2012. Tests for Geometrical Properties of Aggregates - Part 1: Determination of Particle Size Distribution - Sieving Method.

E.N. 933-3:2012, 2017. Tests for Geometrical Properties of Aggregates - Part 3: Determination of Particle Shape - Flakiness Index.

Esveld, C., 2003. Recent developments in slab track. Eur. Railw. Rev. 9, 81–85.

Etxeberria, M., Vázquez, E., Marí, A., Barra, M., 2007. Influence of amount of recycled coarse aggregates and production process on properties of recycled aggregate concrete. Cement Concr. Res. 37, 735–742. https://doi.org/10.1016/j.cemconres.2007.02.002.

Evangelista, L., de Brito, J., 2010. Durability performance of concrete made with fine recycled concrete aggregates. Cement Concr. Compos. 32, 9–14. https://doi.org/10.1016/j.cemconcomp.2009.09.005.

Fomento, M., 2008. Instrucción de Hormigón Estructural EHE-08. Fomento, Madrid, España. https://doi.org/10.1017/CBO9781107415324.004.

Ho, N.Y., Lee, Y.P.K., Lim, W.F., Zayed, T., Chew, K.C., Low, G.L., Ting, S.K., 2013. Efficient utilization of recycled concrete aggregate in structural concrete. J. Mater. Civ. Eng. 25, 318–327. https://doi.org/10.1061/(ASCE)MT.1943-5533.0000587.
Júnior, N.S.A., Silva, G.A.O., V Ribeiro, D., 2017. Effects of the incorporation of recycled aggregate in the durability of the concrete submitted to freeze-thaw cycles. Constr. Build. Mater.
Kou, S.C., Poon, C.S., 2009. Properties of self-compacting concrete prepared with coarse and fine recycled concrete aggregates. Cement Concr. Compos. 31, 622–627.
Kou, S.C., Poon, C.S., 2012. Enhancing the durability properties of concrete prepared with coarse recycled aggregate. Constr. Build. Mater. 35, 69–76. https://doi.org/10.1016/J.CONBUILDMAT.2012.02.032.
Kou, S.C., Poon, C.S., Dixon, C., 2007. Influence of fly ash as cement replacement on the properties of recycled aggregate concrete. J. Mater. Civ. Eng. 19, 709–717. https://doi.org/10.1061/(ASCE)0899-1561(2007)19:9(709).
Laplante, P., Aïtcin, P.C., Vézina, D., 1991. Abrasion resistance of concrete. J. Mater. Civ. Eng. 3, 19–28. https://doi.org/10.1061/(ASCE)0899-1561(1991)3:1(19).
M. de fomento 7735, 2006. Requisitos para el balasto, pp. 16891–16909.
Matias, D., de Brito, J., Rosa, A., Pedro, D., 2014. Durability of concrete with recycled coarse aggregates: influence of superplasticizers. J. Mater. Civ. Eng. 26 https://doi.org/10.1061/(ASCE)MT.1943-5533.0000961.
Medina, C., Zhu, W., Howind, T., Sánchez de Rojas, M.I., Frías, M., 2014. Influence of mixed recycled aggregate on the physical – mechanical properties of recycled concrete. J. Clean. Prod. 68, 216–225. https://doi.org/10.1016/J.JCLEPRO.2014.01.002.
F.F. Oliván, Estudio experimental sobre propiedades mecánicas y de durabilidad de hormigones estructurales autocompactantes con áridos reciclados y su aplicación a la prefabricación, n.d.
Omary, S., Ghorbel, E., Wardeh, G., 2016. Relationships between recycled concrete aggregates characteristics and recycled aggregates concretes properties. Constr. Build. Mater. 108, 163–174.
Padmini, A.K., Ramamurthy, K., Mathews, M.S., 2009. Influence of parent concrete on the properties of recycled aggregate concrete. Constr. Build. Mater. 23, 829–836.
Pereira-De-Oliveira, L.A., Nepomuceno, M.C.S., Castro-Gomes, J.P., Vila, M.F.C., 2014. Permeability properties of self-Compacting concrete with coarse recycled aggregates. Constr. Build. Mater. 51, 113–120. https://doi.org/10.1016/j.conbuildmat.2013.10.061.
Poon, C.-S., Chan, D., 2007. The use of recycled aggregate in concrete in Hong Kong. Resour. Conserv. Recycl. 50, 293–305. https://doi.org/10.1016/j.resconrec.2006.06.005.
Poon, C.S., Kou, S.C., Lam, L., 2002. Use of recycled aggregates in molded concrete bricks and blocks. Constr. Build. Mater. 16, 281–289.
Ravindrarajah, R.S., Loo, Y.H., Tam, C.T., 1987. Recycled concrete as fine and coarse aggregates in concrete. Mag. Concr. Res. 39, 214–220.
Richardson, A., Coventry, K., Bacon, J., 2011. Freeze/thaw durability of concrete with recycled demolition aggregate compared to virgin aggregate concrete. J. Clean. Prod. 19, 272–277. https://doi.org/10.1016/J.JCLEPRO.2010.09.014.
Saravana Kumar, P., Dhinakaran, G., 2012. Effect of admixed recycled aggregate concrete on properties of fresh and hardened concrete. J. Mater. Civ. Eng. 24, 494–498. https://doi.org/10.1061/(ASCE)MT.1943-5533.0000393.
She, W., Du, Y., Zhao, G., Feng, P., Zhang, Y., Cao, X., 2018. Influence of coarse fly ash on the performance of foam concrete and its application in high-speed railway roadbeds. Constr. Build. Mater. 170, 153–166.
Silva, R.V., De Brito, J., Dhir, R.K., 2014. Properties and composition of recycled aggregates from construction and demolition waste suitable for concrete production. Constr. Build. Mater. 65, 201–217.
Soares, D., de Brito, J., Ferreira, J., Pacheco, J., 2014. Use of coarse recycled aggregates from precast concrete rejects: mechanical and durability performance. Constr. Build. Mater. 71, 263–272. https://doi.org/10.1016/J.CONBUILDMAT.2014.08.034.
Standards Australia, 2009. Reinforced Concrete Design.
Tabsh, S.W., Abdelfatah, A.S., 2009. Influence of recycled concrete aggregates on strength properties of concrete. Constr. Build. Mater. 23, 1163–1167. https://doi.org/10.1016/J.CONBUILDMAT.2008.06.007.
Tayabji, S., Bilow, D., 2001. Concrete slab track state of the practice. Transp. Res. Rec. J. Transp. Res. Board. 1742, 87–96.
Thomas, C., Setién, J., Polanco, J.A.Ja, Alaejos, P., De Juan, M.S., Sánchez de Juan, M., 2013. Durability of recycled aggregate concrete. Constr. Build. Mater. 40, 1054–1065. https://doi.org/10.1016/J.CONBUILDMAT.2012.11.106.
Thomas, C., Setién, J., Polanco, J.A., 2016. Structural recycled aggregate concrete made with precast wastes. Constr. Build. Mater. 114, 536–546. https://doi.org/10.1016/j.conbuildmat.2016.03.203.
Tosti, L., van Zomeren, A., Pels, J.R., Comans, R.N.J., 2018. Technical and environmental performance of lower carbon footprint cement mortars containing biomass fly ash as a secondary cementitious material. Resour. Conserv. Recycl. 134, 25–33. https://doi.org/10.1016/J.RESCONREC.2018.03.004.
U.-E. 12390-3:2009, 2009. Testing Hardened Concrete - Part 3: Compressive Strength of Test Specimens.
U.-E. 12390-8:2009/1M:2011, 2011. Testing Hardened Concrete - Part 8: Depth of Penetration of Water under Pressure.
U.N.E. 80103:2013, 2013. Test Methods of Cements. Physical Analysis. Actual density determination.
U.N.E. 83318:1994, 1994. CONCRETE TESTS. DETERMINATION OF THE LENGTH CHANGES.
U.N.E. 83966:2008, 2008. Concrete Durability. Test Methods. Conditioning of Concrete Test Pieces for the Purpose of Gas Permeability and Capilar Suction Tests.
U.N.E. 83980:2014, 2014. Concrete Durability. Test Methods. Determination of the Water Absorption, Density and Accessible Porosity for Water in Concrete.
U.N.E. 83981:2008, 2008. Concrete Durability. Test Methods. Determination to Gas Permeability of Hardened Concrete.
U.N.E. 83981:2008, 2011. ERRATUM:2011, Concrete Durability. Test Methods. Determination to Gas Permeability of Hardened Concrete.
Uthaman, S., Vishwakarma, V., George, R.P., Ramachandran, D., Kumari, K., Preetha, R., Premila, M., Rajaraman, R., Mudali, U.K., Amarendra, G., 2018. Enhancement of strength and durability of fly ash concrete in seawater environments: synergistic effect of nanoparticles. Constr. Build. Mater. 187, 448–459. https://doi.org/10.1016/J.CONBUILDMAT.2018.07.214.
Warudkar, A., Elavenil, S., Arunkumar, A., 2018. Assessment of abrasion resistance of concrete pavement for durability. Int. J. Civ. Eng. Technol. 9, 1176–1181. https://www.scopus.com/inward/record.uri?eid=2-s2.0-85049592297&partnerID=40&md5=c94d2d3045019182ccab201a1e1917d9.
Xiao, J., Wang, C., Ding, T., Akbarnezhad, A., 2018. A recycled aggregate concrete high-rise building: structural performance and embodied carbon footprint. J. Clean. Prod. 199, 868–881. https://doi.org/10.1016/J.JCLEPRO.2018.07.210.
Zega, C.J., Di Maio, Á.A., 2011. Use of recycled fine aggregate in concretes with durable requirements. Waste Manag. 31, 2336–2340. https://doi.org/10.1016/j.wasman.2011.06.011.
Zega, C.J., Villagrán-Zaccardi, Y.A., Di Maio, A.A., 2010. Effect of natural coarse aggregate type on the physical and mechanical properties of recycled coarse aggregates. Mater. Struct. Constr. 43, 195–202. https://doi.org/10.1617/s11527-009-9480-4.